Contribution from the Institute of General and Inorganic Chemistry, Bulgarian Academy of Science, 1040 Sofia, Bulgaria, and Institut für Theoretische Chemie, Heinrich-Heine-Universität Düsseldorf, Universitätsstrasse 1, D-4000 Düsseldorf, FRG

The Role of π-Bonding for Trigonal Level Splittings in Chelate Complexes. 3. The Lowest Electronic States in $Cr(acac)_3$[†]

Michail Atanasov[‡] and Thomas Schönherr*[,§]

Received February 23, 1990

The $^2E_g \rightarrow {}^4A_{2g}$ polarized emission spectra of Cr(III)-doped $Ga(acac)_3$ were measured down to 1.9 K in the region of the zero-phonon transitions. Zero-field ground-state splitting could be optically resolved to 1.1–1.2 cm^{-1} for the four inequivalent $Cr(acac)_3$ molecules in the host crystal. Polarization ratios and dipole oscillator strengths for D_3* symmetry show $2\bar{A}$ (^2E_g) as the lowest emitting state. A large trigonal ^2E_g splitting of about 250 cm^{-1} was obtained from absorption measurements. These results were rationalized in terms of an extended angular overlap model, which considers specific π interactions between metal d and chelate-ring π orbitals and the detailed angular geometry simultaneously. From calculations for $Cr(acac)_3$ the π-bonding effects were found to be the main source for the sign and magnitude of the observed excited-state splittings, whereas the ground-state splitting is very sensitive to the angular geometry and the anisotropic spin–orbit coupling. Theoretical results obtained by introducing the Zeeman operator are consistent with the experimental findings obtained from Zeeman spectra reported previously. We have also checked the concept of misdirected valency, which considers the orientation of the oxygen lone pairs with respect to the metal–ligand bonding axes. However, with the introduction of σ–π mixing as reported for other $acac^-$ complexes, a level sequence was calculated, which is in variance with our polarized spectra.

Introduction

The assignment of the lowest emitting state in $Cr(acac)_3$ has been subject to a longstanding controversy. Different explanations of the observed three prominent phosphorescence bands in $Al(acac)_3$:Cr^{3+} have been given: the early assignment of Courtois and Forster (two electronic origins accompanied by one intense lattice mode[3]) has been refuted by a temperature study of absorption and emission spectra interpreting these bands with reference to the same zero-phonon origin due to different chromium sites in the low-temperature phase,[4] which later was confirmed by a site-selective phosphorescence study.[5] The nature of the emitting state is still not clear: From ligand field calculations, which can reproduce the experimental level scheme fairly well, a $2\bar{A}$ (^2E_g) lowest excited electronic state with a trigonal ^2E_g splitting >200 cm^{-1} must be expected[4] [the notation for the considered Kramers doublets is given here within the trigonal double group D_3* (O_h for the parent Russell–Saunders terms in an octahedral field)]. On the other hand, Fields et al.[5,6] have assigned the emitting state from Zeeman splittings of the considered Kramers doublets to be an $\bar{E}$ ($^2T_{1g}$) for the reason that the $g_\perp$, $g_\parallel$ values of the lowest excited state exhibit an opposite relationship when compared to those of ruby. However, the quality of both assignments suffers from the fact that inadequate wave functions are implicitly used; i.e. the obtained trigonal ligand field parameters K and K' based on a ^2E_g emitting state[4] lead to a nonphysical value for the related parameter η [$=(\langle r^2\rangle/\langle r^4\rangle)R^2$],[7] whereas in the other case ($^2T_{1g}$ emitter) the neglect of effects due to the different natures of the Cr–O bonding in $Cr(acac)_3$ and ruby[5] must be criticized (vide infra).

In this particle we report highly resolved polarized emission spectra of Cr^{3+}-doped $Ga(acac)_3$. This system seems to be more appropriate for such an investigation than $Al(acac)_3$:Cr^{3+}, where disadvantageous orientations of the molecular trigonal axes due to crystallographically nonequivalent chromium sites in the Al lattice prevent more significant polarization effects in the optical spectra. An EPR study of $Ga(acac)_3$–Cr^{3+} shows almost axial spectra with a g tensor and a zero-field splitting (ZFS) of the ground state[8] very close to the values reported for other host materials (M = Al^{3+}, Co^{3+}).[9] Since the sign of the ZFS is already known,[6] a way of unambiguously assigning the emitting state is offered by the analysis of polarized optical spectra.

The spectroscopic results will be discussed in the framework of an angular overlap model (AOM), which also considers *phase coupling* of the molecular orbitals on the chelate ligand.[1,2,11–13] This extension leads to nonadditive contributions to the d-orbital energies due to three-center orbital interactions. Since this model is able to explain the quartet-level schemes of chromium tris(acetylacetonate) and tris(oxalate),[1] it should be also applicable for predictions within the series of the experimentally observed doublet states. Here, we elaborate the AOM for trigonal chelate complexes in further detail by considering the explicit angular geometry in a full d^3 calculation that includes the electrostatic interaction, spin–orbit coupling, and an external magnetic field simultaneously. Especially, attention will be paid to the question of how π-bonding and trigonal geometric distortions influence the sign and magnitude of the low-energy-level splittings in these complexes.

We will also compare our results with an alternative approach that considers the mixing of σ and π contributions due to the misaligned orientations of ligand orbitals. Following an idea of Liehr,[13] the concept of *misdirected valency* was first introduced into the AOM formalism by Gerloch et al.,[14,15] who suggested that this effect, rather than phase coupling, determines the band splittings in chelate complexes. The title compound, $Cr(acac)_3$, for which spectral and structural data are carefully collected, can serve as a model complex to test these two different concepts.

Experimental Section

$Cr(acac)_3$ and the isomorphic gallium compound were synthesized by using standard methods.[16] Mixed single crystals were grown by slow evaporation from acetone solutions at room temperature containing various amounts of the two compounds. Crystals containing between 0.1 and 1–2 mol % Cr exhibited no qualitative differences in the optical properties; e.g. crucial Cr–Cr interactions can be neglected in the following discussion.

[†] For parts 1 and 2 in this series, see refs 1 and 2.
[‡] Bulgarian Academy of Science.
[§] Heinrich-Heine-Universität Düsseldorf.

(1) Atanasov, M. A.; Schönherr, T.; Schmidtke, H.-H. *Theor. Chim. Acta* **1987**, *71*, 59.
(2) Schönherr, T.; Atanasov, M. A.; Schmidtke, H.-H. *Inorg. Chim. Acta* **1988**, *141*, 27.
(3) Courtois, M.; Forster, L. S. *J. Mol. Spectrosc.* **1965**, *18*, 396.
(4) Schönherr, T.; Eyring, G.; Linder, R. *Z. Naturforsch., Teil A* **1983**, *38*, 736.
(5) Fields, R. A.; Winscom, C. J.; Haindl, E.; Plato, M.; Möbius, K. *Chem. Phys. Lett.* **1986**, *124*, 121.
(6) Fields, R. A.; Haindl, E.; Winscom, C. J.; Kahn, Z. H.; Plato, M.; Möbius, K. *J. Chem. Phys.* **1984**, *80*, 3082.
(7) Schoenen, N.; Schmidtke, H.-H. *Mol. Phys.* **1986**, *57*, 983.
(8) Elbers, G.; Remme, S.; Lehmann, G. *Inorg. Chem.* **1986**, *25*, 896.
(9) Andriessen, W. T. M. *J. Phys. Chem. Solids* **1976**, *37*, 189.
(10) Orgel, L. E. *J. Chem. Soc.* **1961**, 3683.
(11) Ceulemans, A.; Dendooven, M.; Vanquickenborne, L. G. *Inorg. Chem.* **1985**, *24*, 1153.
(12) Ceulemans, A.; Bongaerts, N.; Vanquickenborne, L. G. In *Photochemistry and Photophysics of Coordination Compounds*; Yersin, H., Vogler, A., Eds.; Springer: Berlin, 1987; p 31.
(13) Liehr, A. D. *J. Phys. Chem.* **1964**, *68*, 665.
(14) Deeth, R. J.; Duer, M. J.; Gerloch, M. *Inorg. Chem.* **1987**, *26*, 2573.
(15) Deeth, R. J.; Duer, M. J.; Gerloch, M. *Inorg. Chem.* **1987**, *26*, 2578.
(16) Gmelin. *Handbuch der anorganischen Chemie*; Springer: Berlin; Vols. 25 and 52.

0020-1669/90/1329-4545$02.50/0

d_{z^2}	d_{yz}	d_{xz}	d_{xy}	$d_{x^2-y^2}$
$e_\sigma/2$	0	0	0	$(\sqrt{3}/2)(\cos\alpha)e_\sigma$
	$2\cos^2(\alpha/2)e_{\pi s}$	0	0	0
		$2\sin^2(\alpha/2)e'_{\pi s}$	0	0
			$(3/2)(\sin^2\alpha)e_\sigma + 2(\cos^2\alpha)e_{\pi c}$	0
				$(3/2)(\cos^2\alpha)e_\sigma + 2(\sin^2\alpha)e_{\pi c}$

(2)

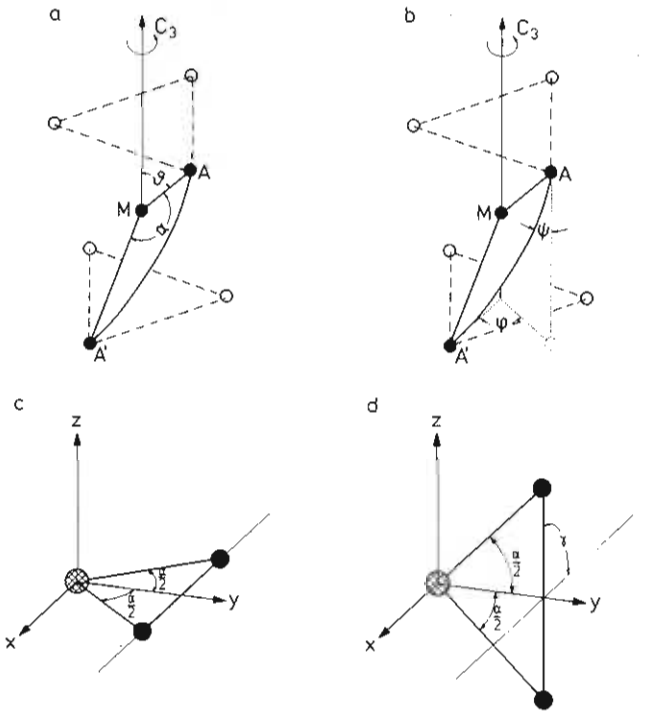

Figure 1. (a, b) Structural angles for a tris bidentate $M(A-A)_3$ complex. (c, d) Coordinate axes orientation for one chelate ligand in the general position. In order to generate the full symmetry, two further rotations of the ligand by an angle of ±120° around the z axis are necessary.

Highly resolved spectra in absorption and emission were recorded with a McPherson 0.5-m double monochromator and a red-sensitive GaAs photomultiplier. Temperatures down to 1.9 K were achieved with use of a helium bath cryostat. Polarized measurements were carried out by using Glan–Taylor prisms or sheet polarizers with the light perpendicular to the ab plane and the E vector parallel and perpendicular to the crystallographic b axis,[17] which was easily determined under a polarizing microscope.

Trigonal AOM Matrix

(a) The Phase-Coupling Concept. The angular geometry for a $M(A-A)_3$ complex of D_3 symmetry (A–A represents a symmetrically coordinated bidentate ligand) can be uniquely described by two structural angles (cf. Figure 1a,b): the polar angle ϑ and the twisting angle φ, assuming at $\varphi = 0°$ and $\varphi = 60°$ the higher symmetry arrangements of a trigonal prism (D_{3h}) and a trigonal antiprism (D_{3d}), respectively. A regular octahedral geometry of the MA_6 chromophore yields $\vartheta_{O_h} = 54.74°$ and $\varphi_{O_h} = 60°$. Variation of ϑ describes a compression ($\vartheta > \vartheta_{O_h}$) or elongation ($\vartheta < \vartheta_{O_h}$) along the trigonal axis. Other structural angles, i.e. the ligand bite angle $\alpha = \angle AMA$ and the dihedral angle ψ, the latter defined by the angle between the AMA chelate plane and the plane containing the trigonal axis C_3 and the M–A bond vector, are not independent of ϑ and φ:[1]

$$\cos\psi = \cos\vartheta\cos(\varphi/2)/\sin(\alpha/2)$$
$$\cos(\alpha/2) = \sin\vartheta\cos(\varphi/2) \qquad (1)$$

The AOM perturbation matrix for a trigonal complex with ligand atoms located on the coordinate axes has been previously derived.[1,11] For a general arrangement of D_3 symmetry, both angles ϑ and φ have to be considered and, additionally, the angle ψ is explicitly introduced into the AOM expressions, since π interactions for in-plane ($e_{\pi c}$) and out-of-plane ($e_{\pi s}$) orbitals are essentially different.

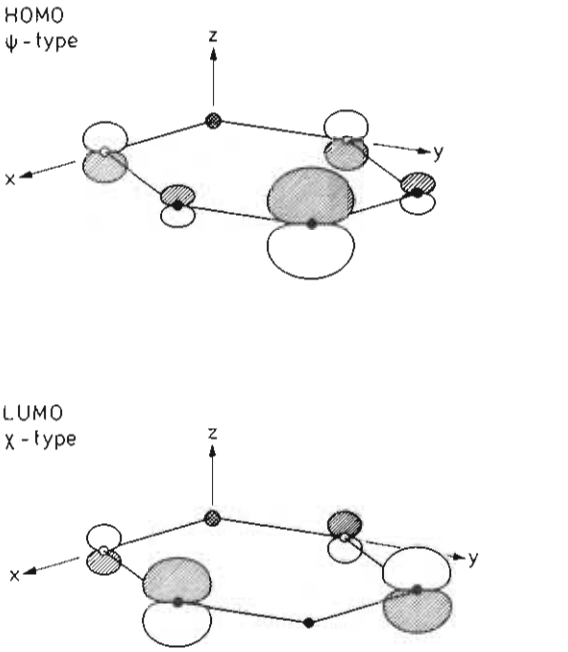

Figure 2. HOMO and LUMO orbitals of acac as obtained from a Hückel calculation, using parameters from ref 18.

A further distinction within the out-of-plane interactions originates from a specific phase relation of ligand π orbitals, which commonly have different energies and thus contribute to a different extent to the antibonding energies of metal d orbitals. The phase coupling (nonadditive) model distinguishes between two out-of-plane π-bond parameters, one ($e_{\pi s}$) for in-phase coupling and another one ($e'_{\pi s}$) for out-of-phase coupling.[1] The former mechanism applies if the atomic orbital coefficients of the relevant molecular orbitals of the chelate have equal signs; in the other case out-of-phase coupling is operative. In the case of $Cr(acac)_3$ these parameters are related to the HOMO ($e_{\pi s}$) and LUMO ($e'_{\pi s}$) frontier orbitals, respectively, which are given in Figure 2.

The AOM matrix for a general D_3 geometry that accounts for these effects can be obtained by starting from a reference position of the metal and one bidentate ligand, as depicted in Figure 1c. For this arrangement the symmetric matrix $\mathcal{E}$ can be shown to have the simple form shown in eq 2. In order to locate the ligand into its position in the trigonal complex, a rotation by an angle γ around the y axis is performed (Figure 1d). γ can be expressed in terms of ϑ and φ as follows:

$$\cos\gamma = \sin\vartheta\sin(\varphi/2)/\sin(\alpha/2) = \cos\psi\tan\vartheta\tan(\varphi/2) \qquad (3)$$

where $0 \le \gamma \le 90$, $0 \le \vartheta \le 90$, and $0 \le \varphi \le 60°$.

This specific choice enables us to avoid introducing the angle ψ into the formalism, since for a planar chelate ligand the value of ψ is given by defining the AMA plane. Then the matrix $\mathcal{E}$ is transformed into

$$\mathbf{A} = \mathbf{D}_y(\gamma)\,\mathcal{E}\,\tilde{\mathbf{D}}_y(\gamma) \qquad (4)$$

where $\mathbf{D}_y(\gamma)$ is given by eq 5.[19]

(17) Astbury, W. T. *Proc. R. Soc.* **1926**, *112*, 448.
(18) Pullman, B.; Pullman, A. *Quantum Biochemistry*; Interscience: New York, 1963.

$$D_y(\gamma) = \begin{bmatrix} (1/4)(1+3\cos(2\gamma)) & 0 & -(\sqrt{3}/2)\sin(2\gamma) & 0 & (\sqrt{3}/4)(1-\cos(2\gamma)) \\ 0 & \cos\gamma & 0 & -\sin\gamma & 0 \\ (\sqrt{3}/2)\sin(2\gamma) & 0 & \cos(2\gamma) & 0 & -(1/2)\sin(2\gamma) \\ 0 & \sin\gamma & 0 & \cos\gamma & 0 \\ (\sqrt{3}/4)(1-\cos(2\gamma)) & 0 & (1/2)\sin(2\gamma) & 0 & (1/4)(3+\cos(2\gamma)) \end{bmatrix} \quad (5)$$

Table I. Squared Dipole Oscillator Strengths of the $^4A_{2g} \leftrightarrow {}^2E_g, {}^2T_{1g}$ Transitions for Trigonal Symmetry[a]

	$2\bar{A}(\pm^1/_2u_\pm)$	$\bar{E}(\pm^1/_2u_\mp)$	$\bar{E}^a(\pm^1/_2a_\mp)$	$2\bar{A}(\pm^1/_2a_\mp)$	$\bar{E}^b(\pm^1/_2a_0)$
$2\bar{A}(\pm^3/_2)$	π	σ	σ_0	$\bar{\pi}$	σ'
$\bar{E}(\pm^1/_2)$	σ	$^2/_3\sigma + {}^1/_3\pi$	$^2/_3\bar{\sigma} + {}^1/_3\bar{\pi}$	$^2/_3\bar{\sigma} + {}^1/_3\sigma_0$	$^2/_3\sigma' + {}^1/_3\pi'$

[a] The parametrization follows that presented in ref 23.

The trigonal molecular arrangement is completed by rotations of the ligand by ±120° around the z axis, yielding the full expression for the AOM matrix:

$$A_{trig} = A + D_z(120°)\, A\, \tilde{D}_z(120°) + D_z(-120°)\, A\, \tilde{D}_z(-120°) \quad (6)$$

where

$$D_z(\pm 120°) = \begin{bmatrix} 1 & 0 & 0 & 0 & 0 \\ 0 & -1/2 & \pm\sqrt{3}/2 & 0 & 0 \\ 0 & \mp\sqrt{3}/2 & -1/2 & 0 & 0 \\ 0 & 0 & 0 & -1/2 & \mp\sqrt{3}/2 \\ 0 & 0 & 0 & \pm\sqrt{3}/2 & -1/2 \end{bmatrix} \quad (7)$$

(b) The Concept of Misdirected Valency. An alternative or possibly supplementary way to look at the electronic structure of acetylacetonate complexes concerns the local pseudosymmetry of the M–O bond, which may be C_s or even lower rather than C_{2v}.[14] This is due to the oxygen sp^2 lone pair and to the rigidity of the chelate ligand preventing a separation into electronic densities for pure σ and π interactions.[15] Thus the AOM matrix for a ligator atom located on the z axis is no longer diagonal and takes the form

d_{z^2}	d_{xz}	d_{yz}
e_σ	$e_{\sigma\pi c}$	$e_{\sigma\pi s}$
$e_{\sigma\pi c}$	$e_{\pi c}$	0
$e_{\sigma\pi s}$	0	$e_{\pi s}$

(8)

where the new parameters $e_{\sigma\pi c}$ and $e_{\sigma\pi s}$ account for the mixing of d orbitals due to the misaligned ligand orbitals in the mean chelate plane and perpendicular to it, respectively.[14] For a ligand in the general position, one can employ the matrix rotation technique, and the AOM matrix, which corresponds to a chelate ligand as shown in Figure 1c, can be obtained by two consecutive rotations of 90° around the y axis, followed by a rotation of 90° ± $\alpha/2$ around z. The resulting matrix is now given by eq 9. From this expression, the trigonal ligand field matrix can be generated in the same way as for the phase coupling matrix by using eqs 4–7.

The AOM matrices of both concepts were implemented into a program that enables full account of electronic repulsion, spin–orbit coupling, and Zeeman energy for systems of d^n configurations.

Optical Spectra

The zero-phonon region of the single-crystal polarized emission spectrum of $Ga(acac)_3:Cr^{3+}$ is depicted in Figure 3. It clearly shows four prominent lines, each of them optically resolved into two components that are separated from each other by 1.2 cm^{-1}. This value exactly corresponds to the ZFS of the $^4A_{2g}$ ground state, as obtained from previous EPR studies on $Cr(acac)_3$ in various host lattices.[8,9] The appearance of four similar bands in the electronic spectrum is consistent with the EPR results of the same system, which revealed up to four closely spaced signals arising from nonequivalent centers with slightly different EPR parameters.[20] However, both spectroscopic measurements are at variance with the known structural data of $Ga(acac)_3$,[21] which suggest 4 molecules/unit cell being equivalent for reasons of symmetry in the monoclinic space group $P2_1/c$ (C_{2h}^5). A structural change to a phase transition when crystals were cooled down to helium temperatures, as is the case for the isomorphic $Al(acac)_3$,[9] was not substantiated by an analysis of the EPR lines in the temperature range 300–20 K,[8] and the emission band pattern is not changed with respect to the existence of four well-separated zero-phonon lines within the temperature range 50–1.9 K (at higher temperatures band broadening prevents the localization of distinct transitions). The appearance of additional spectral features due to exchange-coupled chromium ions was excluded by concentration-dependent optical measurements and the EPR data likewise. A plausible explanation for the discrepancy between structural and spectroscopic results, on the other hand, is offered by the limited resolution of the X-ray data in the presence of heavy-metal atoms, and additional difficulties arise in the present case from the unusually large thermal motion of certain methyl groups.[21,22]

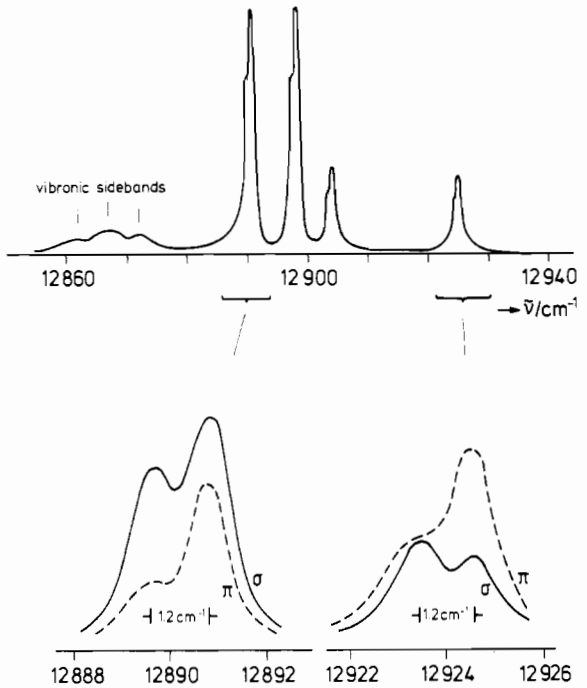

Figure 3. High-resolution polarized emission spectrum of $Ga(acac)_3$ doped with 0.1% Cr^{3+} in the zero-phonon region (T = 1.9 K).

Since the direction of each trigonal axis is close to the crystallographic b axis, considerable polarization effects due to the zero-phonon transitions are expected. Since the α-spectrum coincides with the σ-spectrum and is different from the π-spectrum, the measured band intensities are primarily due to an electric dipole mechanism. The squared dipole oscillator strengths of the $^4A_{2g} \leftrightarrow {}^2E_g, {}^2T_{1g}$ transitions for trigonal symmetry have been determined previously[23] and are presented in Table I. They are

(19) Schaeffer, C. E. *Struct. Bonding (Berlin)* **1968**, *5*, 68.
(20) Elbers, G. Dissertation, Universität Münster, 1987.
(21) Dymock, K.; Palenic, G. J. *Acta Crystallogr.* **1974**, *B30*, 1364.
(22) Morosin, B. *Acta Crystallogr.* **1965**, *19*, 131.
(23) Sugano, S.; Tanabe, Y. *J. Phys. Soc. Jpn.* **1958**, *13*, 880.

d_{z^2}	d_{yz}	d_{xz}	d_{xy}	$d_{x^2-y^2}$
$e_\sigma/2$	$e_{\sigma\pi s}\cos(\alpha/2)$	0	0	$(\sqrt{3}/2)e_\sigma\cos\alpha - e_{\sigma\pi c}\sin\alpha$
	$2e_{\pi s}\cos^2(\alpha/2)$	0	0	$\sqrt{3}e_{\sigma\pi s}\cos\alpha\cos(\alpha/2)$
		$2e_{\pi s}\sin^2(\alpha/2)$	$-\sqrt{3}e_{\sigma\pi s}\sin\alpha\sin(\alpha/2)$	0
			$(3/2)e_\sigma\sin^2\alpha + 2e_{\pi c}\cos^2\alpha + \sqrt{3}e_{\sigma\pi c}\sin(2\alpha)$	0
				$(3/2)e_\sigma\cos^2\alpha + 2e_{\pi c}\sin^2\alpha - \sqrt{3}e_{\sigma\pi c}\sin(2\alpha)$

(9)

given in terms of the quantities σ, π ($^2\Gamma = {}^2E_g$) and $\bar{\sigma}$, $\bar{\pi}$, σ_0, σ', π' ($^2\Gamma = {}^2T_{1g}$), which parametrize expressions of the form

$$\frac{(^4A_{2g}|\mathbf{P}|^4\Gamma')(^4\Gamma'|V_{SO}|^2\Gamma)}{W(^2\Gamma) - W(^4\Gamma')} \qquad (10)$$

and were explained in detail elsewhere.[23] By measuring the intensities of EPR lines at different temperatures, the sign of the ground-term ZFS was determined to be negative (i.e. $D < 0$), leading to $2\bar{A}$ ($\pm^3/_2$) < $\bar{E}$ ($\pm^1/_2$).[8] The emission spectrum clearly shows that the lower energy component of each zero-phonon line is predominantly σ-polarized ($\mathbf{E}\perp C_3$), whereas the higher energy transition is π-polarized ($\mathbf{E}\parallel C_3$) (cf. Figure 3). Since a splitting pattern $\bar{E}^a < 2\bar{A} < \bar{E}^b$ is generally obtained for the $^2T_{1g}$ state (vide infra), it follows from the electric dipole selection rules (cf. Table I) that the observed polarizations of the zero-phonon lines are only consistent with a $2\bar{A}$ emitting state originating from ^2E_g. Other possible assignments, e.g. to a level of $\bar{E}$ symmetry (originating from either ^2E_g or $^2T_{1g}$), as proposed by Fields et al.,[5] would afford a significant σ contribution in the higher energy components, which is, however, at variance with the experimentally observed polarizations. Moreover, our assignments are also consistent with the Zeeman level splittings and the intensities of phosphorescence bands at various strengths of the magnetic field, as given in ref 6: the transition $-^1/_2u_-(2\bar{A}) \rightarrow {}^3/_2(2\bar{A})$ of lowest energy is expected to be forbidden in accordance with the weak emission line observed at the low-energy end of the spectrum. The other three split components of increasing energy are $-^1/_2u_-(2\bar{A}) \rightarrow {}^1/_2(\bar{E})$, $\rightarrow -^1/_2(\bar{E})$, and $\rightarrow -^3/_2(2\bar{A})$ with intensities $\sigma/6$, $\sigma/3$, and $\pi/2$, respectively. Since the bands are more intense for the π polarization, the Zeeman-split component of highest energy is expected to be the most pronounced (π) when compared to the remaining two lines (σ). This is again in agreement with the experimental band pattern. Therefore, we can conclude from the polarized emission spectra in accordance with the data from magnetic measurements that ^2E_g splits in the trigonal field with a term sequence $2\bar{A}$(emitting state) < $\bar{E}$. The magnitude of the ^2E_g splitting varies slightly in the range of 220–290 cm^{-1} for the nonequivalent molecules in the gallium (alumina[4]) host lattice, as obtained from absorbtion measurements of highly doped crystals. This exceeds the ^2E_g splittings in other trigonal chelate complexes observed so far.

Ligand Field Calculations

In order to study the factors that influence the splittings of states with t_{2g}^3 electron configuration, we have performed a series of AOM calculations by diagonalizing the full 120 × 120 perturbation matrix and varying in a systematic way the AOM parameters, the angular geometry (ϑ, φ), the Racah parameters B and C for the electron-electron repulsion, and the parameter ζ, which describes the spin–orbit coupling for the d electrons. From these calculations the actual geometry was found to be of minor importance for the energy separation of the two Kramers doublets resulting from ^2E_g, but it largely influences the splittings of $^2T_{1g}$ and $^4A_{2g}$. On the other hand, the parameters e_σ and $e_{\pi c}$, which account for σ- and π-bonding within the chelate plane, respectively, as well as B and C, do not influence the ^2E_g and $^2T_{1g}$ splittings noticeably.

Following an idea of Orgel,[10] the phase coupling of frontier orbitals of a chelate ligand may cause an additional splitting of the metal t_{2g} orbitals. Since the HOMO for acac is in-phase, i.e. of ψ-type, and the opposite holds for the LUMO, different interactions between these molecular orbitals and the corresponding metal d orbitals are to be expected (cf. Figure 1). This allows for the interpretation of the quartet spectrum[1] and serves here as a starting point for explaining the different sign and magnitude of the trigonal ^2E_g splitting.

Term energies depending on the parameters $e_{\pi s}$ and $e'_{\pi s}$, which reflect the interaction of metal d orbitals to in-phase and out-of-phase ligand π orbitals, respectively, are illustrated in Figure 4. The sign of the ^2E_g splitting determines the way a bidentate ligand couples to the metal, which can be qualitatlvely understood from the relation[22]

$$W[2\bar{A}(^2E_g)] - W[\bar{E}(^2E_g)] = \frac{4}{3}\zeta\frac{\Delta t_2}{W(^2E_g) - W(^4T_{2g})} \qquad (11)$$

where $\Delta t_2 = {}^3/_2(e_{\pi s} - e'_{\pi s})$ represents the energy difference between the e-type and a_1-type d orbitals in a trigonal ligand field. For $Cr(acac)_3$ with relevant in-phase π orbitals ($e_{\pi s} > e'_{\pi s} = 0$), Δt_2 has a positive value, which leads to a level sequence of $2\bar{A} < \bar{E}$.

We note that the effect of phase coupling on the ^2E_g splitting is somewhat larger for in-phase than for out-of-phase coupled

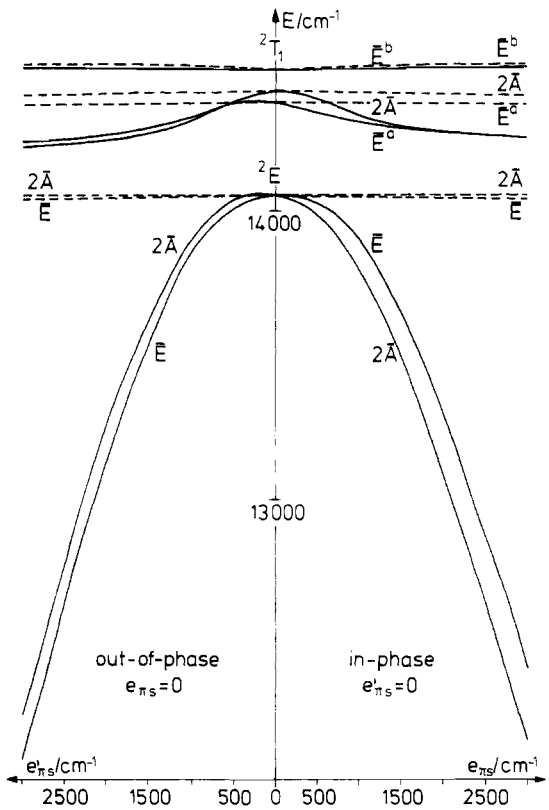

Figure 4. Calculated energy splittings of ^2E_g and $^2T_{1g}$ for in-phase and out-of-phase coupling. Structural angles are $\vartheta = 53.8°$ and $\varphi = 60.8°$; $B = 500$, $C = 3400$, $\zeta = 245$ cm^{-1}. AOM parameters are related by the expressions $3e_\sigma - e'_{\pi s} - 2e_{\pi c} = 18\,700$ cm^{-1} (=$10D_q$) and $e_{\pi c}/e'_{\pi s} = 0.6$. $e'_{\pi s}$ was substituted by $e_{\pi s}$ in the case of in-phase coupling. Broken lines represent term energies when phase coupling is neglected. ($e_{\pi s} = e'_{\pi s}$).

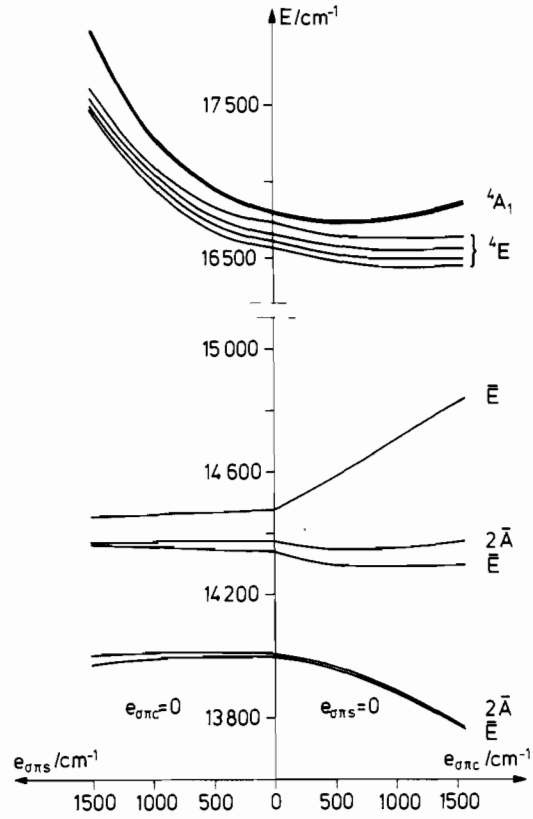

Figure 5. Term energies originating from the octahedral ^2E_g, $^2T_{1g}$, and $^4T_{2g}$ states in the trigonal field as a function of the parameters $e_{\sigma\pi c}$ and $e_{\sigma\pi s}$, which intermix d orbitals of σ- and π-type in an octahedral point symmetry. e_σ = 7700 cm^{-1}; $e_{\pi s}$ ($=e'_{\pi s}$) = 2000 cm^{-1}. The other parameters are given in the legend of Figure 4.

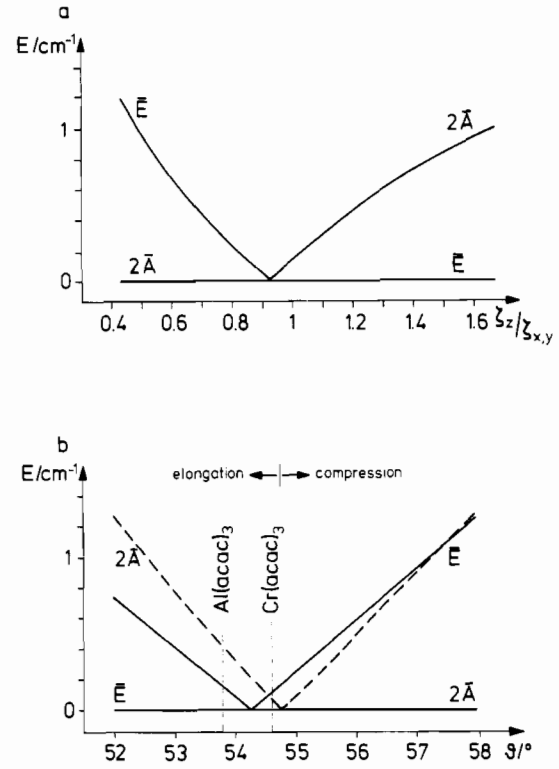

Figure 6. Ground-state splitting for anisotropic spin–orbit coupling (a) and for a trigonal distortion of the CrO_6 chromophore (b). (a) $e_{\pi s} = e'_{\pi s}$. (b) —, in-phase coupling ($e'_{\pi s}$ = 0); - -, no phase coupling ($e_{\pi s} = e'_{\pi s}$). Other parameters are set as for Figure 5.

ligators. The experimental data of $Cr(acac)_3$ show a large splitting indeed (about 250 cm^{-1}), and smaller ones have been reported recently for the out-of-phase coupled 2,2′-bipyridine in different salts of $[Cr(bpy)_3]^{3+}$.[24,25]

The results of a conventional AOM calculation, where phase coupling of ligand π orbitals ($e_{\pi s} = e'_{\pi s}$) is neglected, is also given in Figure 4. The involved angular geometry of the trigonally elongated $Cr(acac)_3$ yields $\bar{E} < 2\bar{A}$, which disagrees with our experimental data; otherwise, this level sequence was really observed for ruby, where the CrO_6 units are also trigonally elongated, but the Orgel effect cannot be operative. As a result, ^2E_g splittings due to trigonal distortions alone (combined with the effect of spin–orbit coupling) are small and counteract to a small extent possible Orgel splittings. Level splittings of other octahedral terms, however, can be much more sensitive with respect to trigonal distortions.

We have also checked the possibility for an alternative explanation of the spectroscopic properties of the $Cr(acac)_3$ complex, using the recently developed concept of *misdirected valency*,[14] where low-symmetry splittings of d orbitals may arise from misaligned ligand orbitals originating from lone pairs or ligand rigidity. This effect leads to a mixing of d orbitals that are exactly of σ and π type, only if an ideal axial symmetry of the metal–ligand bond is given. If this is not the case, two additional parameters, $e_{\sigma\pi c}$ and $e_{\sigma\pi s}$, may describe the σ–π mixing via ligand orbitals parallel and perpendicular to the mean chelate plane. In Figure 5, calculated energy levels of the d^3 electron configuration are given as a function of the orbital mixing parameters $e_{\sigma\pi c}$ and $e_{\sigma\pi s}$; the other parameters were set as for Figure 4. As follows from the almost octahedral geometry of the CrO_6 chromophore with nearly planar chelate ring systems, the mixing parameter $e_{\sigma\pi s}$ must be very close to zero. Therefore, only the right side of the diagram in Figure 5 is of physical relevance for the present complex. The most important result of these calculations, however, is the reverse term sequence for both the $^4T_{2g}$ and the ^2E_g sublevels when compared to the experimentally confirmed level ordering (vide supra). Taking parameter values for $e_{\sigma\pi s}$ and $e_{\sigma\pi c}$ as reported for copper acetylacetonates by Gerloch et al.,[15] again a level ordering for the lowest quartet and doublet states is obtained that is at variance with our spectroscopic data. Consequently, it is seen that the experimental results are favorable with respect to the electronic structure predicted by the phase-coupling concept but are *not* consistent when *only* the model based on the lower local pseudosymmetry is used.

It is worth mentioning that we could not reproduce the relatively large ground-state ZFS $Cr(acac)_3$, even on the basis of the extended AOM model. With use of parameter values as derived from a fit procedure to the spin-allowed bands $^4A_{2g} \rightarrow {}^4T_{2g}$, $^4T_{1g}$ and with consideration of geometries as for various $M(acac)_3$ complexes (M = Al, Ga, Cr), the ZFS parameter $|2D|$ is calculated in either case less than 0.4 cm^{-1}, which is by far too small when compared to the experimental value of $2D = -1.2$ cm^{-1}. Phase coupling, as opposed to trigonal distortions, does not introduce t_{2g}–e_g mixing, which is needed for a large ZFS. The concept of misdirected valency, which considers such a mixing, can also not reproduce the correct sign of $|2D|$ within a reasonable parameter space (with respect to the confirmed excited-state splittings). On the other hand, the explicit use of the spin–orbit coupling operator of the form[23]

$$\mathbf{H}_{\mathcal{LS}} = \zeta_z \mathcal{L}_z \mathcal{S}_z + \zeta_{xy}(\mathcal{L}_x \mathcal{S}_x + \mathcal{L}_y \mathcal{S}_y) \qquad (12)$$

shows that anisotropic spin–orbit coupling quite similar to geometric influences may be of crucial importance for the ground-state splittings, without changing the higher doublet states to a large extent. We were able to restore the correct sign of $|2D|$ when the ζ_z/ζ_{xy} ratio is <0.9 (cf. Figure 6a). However, it is noted that interference with charge-transfer (CT) transitions may also influence the sign and the magnitude of the ZFS in $Cr(acac)_3$. On the other hand, the geometric environment of the Cr^{3+} ion is not exactly known for doped crystals, and O–Cr–O angles may vary over some degrees in different host materials. Thus, the observed

(24) Hauser, A.; Mäder, M.; Robinson, W. T.; Murugesan, R.; Ferguson, J. *Inorg. Chem.* **1987**, *26*, 1331.
(25) Lee, K.-W.; Hoggard, P. E. *Chem. Phys.* **1988**, *135*, 219.

Table II. Calculated Zeeman Splittings and g Factors for $Al(acac)_3:Cr^{3+}$ of the First Excited Doublet State[a]

	in-phase coupling ($e_{\pi s} > e'_{\pi s} = 0$)	no phase coupling ($e_{\pi s} = e'_{\pi s}$)	misdirected valency
$\mathbf{H} \parallel C_3$	$\lvert g_\parallel \rvert = 0.6$	$\lvert g_\parallel \rvert = 2.3$	$\lvert g_\parallel \rvert = 2.6$
$\mathbf{H} \perp C_3$	$\lvert g_\perp \rvert = 0.0$	$\lvert g_\perp \rvert = 0.0$	$\lvert g_\perp \rvert = 0.1$

[a] Experimental g values are for $Cr(acac)_3$ $\lvert g_\parallel \rvert = 1.60$ and $\lvert g_\perp \rvert = 1.921$[5] and for Al_2O_3–Cr^{3+} (ruby) $\lvert g_\parallel \rvert = 2.44$ and $\lvert g_\perp \rvert = 0$.[27]

splitting of the ground-state $^4A_{2g}$ could be explained when a slightly more compressed octahedron is assumed, e.g. by an increase of ϑ by $\approx 2°$ (Figure 6b). Larger trigonal distortions are in fact reasonable for doped compounds in comparison to the pure $Cr(acac)_3$ complex, due to the misfit of the ionic radii (i.e. 64 pm for Cr^{3+} and 57 pm for Al^{3+}).

In the remainder of this section we discuss the unusual behavior of the g values of the emitting state of $Al(acac)_3:Cr$, which have been obtained from optical Zeeman measurements to $\lvert g_\parallel \rvert = 1.60$ and $\lvert g_\perp \rvert = 1.921$.[5] On the basis of this result ($\lvert g_\perp \rvert > \lvert g_\parallel \rvert$), the lowest doublet was assigned to $\bar{E}$ ($\pm^1/_2 a_\pi$) descending from $^2T_{1g}$ by comparing with the g values of ruby, where an opposite relationship ($\lvert g_\perp \rvert < \lvert g_\parallel \rvert$) was observed for both of the split components of the ^2E_g emitting state.[26] It follows from the context of the present discussion, however, that at least due to the phase relation between π orbitals a comparison of $Cr(acac)_3$ to ruby is not allowed.

In order to provide a theoretical basis for further discussions of the Zeeman results, we have introduced the Zeeman operator into the present AOM, starting from the expression

$$H_z = \beta H[(\sin \vartheta_{mag} \cos \varphi_{mag})(\mathcal{L}_x + 2\mathcal{S}_x) + (\sin \vartheta_{mag} \sin \varphi_{mag})(\mathcal{L}_y + 2\mathcal{S}_y) + (\cos \vartheta_{mag})(\mathcal{L}_z + 2\mathcal{S}_z)] \quad (13)$$

With $\beta = 0.4668$ cm^{-1} T^{-1} and ϑ_{mag} and φ_{mag} defining the magnetic field direction, we have calculated the matrix elements of H_z within the basis of real d spin orbitals. With $\vartheta_{mag} = 31°$ and $\varphi_{mag} = 0°$ for H (=5.62 T) parallel to the crystallographic b axis,[21] the luminescent band at 12 932 cm^{-1} is calculated to split into four components, 12 925, 12 929, 12 934, and 12 938 cm^{-1}, in agreement with the experimental values of 12 925.5, 12 930.1, 12 935.1, and 12 941.4 cm^{-1}.[5] These findings reflect both the ground-state $^4A_{2g}$ splitting and the energy shift of the lowest excited state. g values for in-phase coupling ($e_{\pi s} \neq e'_{\pi s} = 0$) and for phase coupling being neglected ($e_{\pi s} = e'_{\pi s}$) are presented in Table II for magnetic field directions parallel and perpendicular to the trigonal axes. They were obtained from level splittings in the magnetic field by use of the expression

$$g_{\perp(\parallel)} = \Delta E_{\perp(\parallel)}/\beta H_{\perp(\parallel)} \quad (14)$$

As a result, the involvement of adequate phase coupling lowers the $\lvert g_\parallel \rvert$ value significantly, although the correct sequence $\lvert g_\perp \rvert > \lvert g_\parallel \rvert$[5] is not derived in either case. Otherwise, the situation known from ruby ($\lvert g_\parallel \rvert \gg \lvert g_\perp \rvert$[27]) is established, which is almost the same as if misdirected valencies of the acetylacetonate ligand are taken into account. This clearly demonstrates the sensitivity of g values with respect to π-bonding pecularities rather than to effects of σ–π mixing due to misaligned ligand orbitals. The former should differ substantially from oxygen ligators like H_2O, OH^-, O^{2-}, ..., due to the intrinsic nature of the π orbitals in the chelate ligand.

Conclusion

As demonstrated by this study, the ligand field spectrum of tris-chelated $Cr(acac)_3$ with conjugated π-electron systems can be substantiated within the angular overlap model when the metal–ligand π-bonding is adequately described. Especially, clarity over the interpretation of the lowest emitting state (i.e. $2\bar{A}$ from ^2E_g) is obtained by an analysis of the polarized emission and Zeeman spectra, which are satisfactorily reproduced when the expected in-phase coupling (ψ-type) of the frontier ligand orbitals (π-donor-type) is considered in the AOM formalism. Otherwise, the concept of misdirected valency, although successfully applied to some cobalt(II) and copper(II) complexes, is not able to describe the correct energy level scheme in $Cr(acac)_3$, for which precise structural and spectroscopic information is available now. Excited-state **g** tensors, however, as well as the unusually large ground-state splitting, are not explained by either approach. This may be caused by interference with charge-transfer states, preventing more precise calculations for these fine effects. Optical Zeeman spectra of related complexes, e.g. changing the π-donor character of the acac ligand by an appropriate substitution of the methyl groups, could give more insight into the still unexplained g behavior of $Cr(acac)_3$ for a better elucidation of the magnetic properties of higher electronic states.

Acknowledgment. We are grateful to Prof. A. Ceulemans, University of Leuven, for helpful discussions and the Deutsche Forschungsgemeinschaft, Bonn, for financial support.

(26) Sugano, S.; Peter, M. *Phys. Rev.* **1961**, *122*, 381.

(27) Terhune, R. W.; Lambe, J.; Kikuchi, C.; Baker, J. *Phys. Rev.* **1961**, *123*, 1265.